Research Square

Preprints are preliminary reports that have not undergone peer review.
They should not be considered conclusive, used to inform clinical practice,
or referenced by the media as validated information.

Estimating the Parameters of the Epileptor Model for Epileptic Seizure Suppression

João Angelo Ferres Brogin (ferres.brogin@unesp.br)
Sao Paulo State University Julio de Mesquita Filho: Universidade Estadual Paulista Julio de Mesquita Filho https://orcid.org/0000-0002-1266-5902

Jean Faber Ferreira de Abreu
Federal University of Sao Paulo: Universidade Federal de Sao Paulo

Douglas Domingues Bueno
Sao Paulo State University Julio de Mesquita Filho: Universidade Estadual Paulista Julio de Mesquita Filho

Research Article

Keywords: Epileptor model, System identification, Parameter estimation, Optimization, Seizure suppression

Posted Date: April 9th, 2021

DOI: https://doi.org/10.21203/rs.3.rs-359235/v1

License: This work is licensed under a Creative Commons Attribution 4.0 International License.
Read Full License

Version of Record: A version of this preprint was published at Neuroinformatics on March 18th, 2022. See the published version at https://doi.org/10.1007/s12021-022-09583-6.

Noname manuscript No.
(will be inserted by the editor)

Estimating the parameters of the Epileptor model for epileptic seizure suppression

João Angelo Ferres Brogin · Jean Faber · Douglas Domingues Bueno

Received: date / Accepted: date

Abstract Epilepsy is one of the most common brain disorders worldwide, affecting millions of people every year. Given the partially successful existing treatments for epileptiform activity suppression, dynamic mathematical models have been proposed with the purpose of better understanding the factors that might trigger an epileptic seizure and how to mitigate it, among which Epileptor stands out, due to its relative simplicity and high prediction ability. Recent studies using such a model have provided evidence that establishing a feedback-based control approach is possible. However, for this strategy to work properly, Epileptor's parameters, which describe the dynamic characteristics of a seizure, must be known beforehand. Therefore, this work proposes a methodology for estimating such parameters based on a successive optimization technique. The results show that it is feasible to approximate their values, and integrating this system identification approach with observers and controllers can be carried out, which might provide an interesting alternative for seizure suppression in practice in the future.

João Angelo Ferres Brogin (corresponding author)
Department of Mechanical Engineering, São Paulo State University (UNESP), School of Engineering of Ilha Solteira, 56 Brasil Avenue, Ilha Solteira, São Paulo, 15385-000, Brazil
Tel.: +55 (18) 3743-1000
ORCID: 0000-0002-1266-5902
E-mail: ferres.brogin@unesp.br

Jean Faber
Department of Neurology and Neurosurgery, Federal University of São Paulo (UNIFESP), 667 Pedro de Toledo Street, São Paulo, São Paulo, 04039-032, Brazil
ORCID: 0000-0002-2129-8251
E-mail: jeanfaber@gmail.com

Douglas Domingues Bueno
Department of Mathematics, São Paulo State University (UNESP), School of Engineering of Ilha Solteira, 56 Brasil Avenue
ORCID: 0000-0002-1783-0524
E-mail: douglas.bueno@unesp.br

Keywords Epileptor model · System identification · Parameter estimation · Optimization · Seizure suppression

1 Introduction

Epilepsy is one of the most severe, intriguing brain disorders worldwide, whose causes, despite possibly linked to genetic abnormalities, centrous nervous system infection, traumas [1] or even external stimuli [2], to name a few, are not fully understood yet [3]. Some of its consequences are: physical implications (increase/decrease of muscle tone, or contraction) [4], physiological implications (headaches, mental confusion or unconsciousness), psychological or psychiatric disorders (as higher incidence of depression and psychosis), and social issues (social dislocation, embarrassment, and isolation) [5]. Therefore, it is a sensitive subject and a major reason for decreasing the quality of life of patients.

Although there are many possible treatments for epilepsy nowadays, such as pharmacological, surgical, based on electrical stimulation [1], neurofeedback [6] and ketogenic diets [7], they, in general, achieve only partially successful results. Understanding the possible epileptogenic mechanisms may, thus, help to clarify the triggering factors of seizures and target the best available treatments. In this sense, mathematical models represent interesting options, especially because one of their main advantages consists in providing a powerful tool for studying physical phenomena (in this case, epilepsy) without necessarily conducting experimental research. This might explain why they have been increasingly well accepted by the scientific community [8].

Nowadays, there exist dynamic models that describe the neural behavior on different scales[1], among which Epileptor stands out when it comes to representing such activity, and, specifically, the main features found in time signatures of seizures, given in terms of local field potentials (LFPs) [15]. Besides providing a greater description of seizure-like events and their possible triggering factors [15], it is a relatively simple, computational and mathematically, easily addressable, and a general-purpose model [17].

Epileptor was developed based on an experimental model using signals obtained from the hippocami of mice, but under the premise that similar dynamic structures are shared across species, which was evidenced by carrying out a detailed statistical analysis of real electrical activity from mice, fish and humans [15]. It has led to many other relevant works, including bifucartion analysis [18], seizure propagation [19], synchronization [20], modulation in phase and frequency [21], and suppression [22][17]. The model can be conveniently written using the state space representation, thus implying in six states and eight parameters, as introduced by [17].

Albeit designed based on biophysical factors [15], Epileptor is composed of rather abstract variables and parameters, which may indicate some restrictions

[1] See, for instance, references [9][10][11][12][13][14][15][16].

for practical usage, such as seizure control. However, Brogin and coauthors [17] introduced a new approach for designing state-feedback-based controllers to suppress epileptic seizures based on this model. The approach considered that all states are known over time, but some of them can not be measured once their physical meaning is not fully established according to current knowledge on this model. Recently, this challenge has been overcome by employing the concept of observality [23], which enabled the development of a state observer for estimating all unmeasured states from only the measurable LFPs [24].

The approaches developed for designing the controller and the state observer make up a powerful tool which allow promising investigations on the use of active control techniques for epileptic seizure suppression. However, for a practical application, it is necessary to establish an Epileptor model to represent each individual for whom an active controller is designed, i.e., customize it. For this case, a specific set of parameters must be defined such that the dynamic responses of the Epileptor model corresponds to the real seizure of the individual. In practice, an Epileptor model must be identified for each individual.

Model and system identification is a widely investigated topic in the literature, encompassing a variety of techniques [25][26]. There are many applications in the fields of engineering. However, applications focused on suppressing epileptic seizures are not found in the literature. Because of this, the main idea in this article is to present an efficient strategy to estimate the parameters involved to describe the Epileptor model. Note that the inter-dependency between controller, observer and a system identification strategy plays a crucial role when conceiving possible therapeutic strategies based on feedback control. In practice, once the parameters of the Epileptor model are properly identified, the gains of the controller and state observer can be accurately computed, as introduced by [17] and [24], respectively.

The approach proposed in this article is based on the optimization algorithm introduced by [27]. However, the algorithm is not directly and simply applied. Therefore, an efficient strategy to obtain the state space representation of the Epileptor model for an individual in epileptic seizure is introduced. The main idea is to measure the LFP during the epileptic seizure and use it as input to the algorithm. The strategy involves a pseudo-random matrix and a normalization criterion to apply the algorithm successively until achieving the best set of parameters to describe the input LFP through the Epileptor model. The results show that it is possible to estimate the Epileptor parameters successfully.

2 Methods

The identification strategy proposed in this article consists of a process with four main stages: *i*) obtaining the input signals (i.e., the LFP), *ii*) pre-optimization, defining initial guesses for the parameters, *iii*) optimization for system identification (modeled as a minimization problem), and *iv*) validation. The third

stage characterizes the optimization itself, during which the unknown parameters of the model are estimated via an objective function based on the LFP. As for the last stage, a validation process is carried out considering several successive optimizations along the LFPs over time, whose median values (as shown herein) tend to converge towards the target ones. Figure 1 depicts an illustration of the aforementioned identification process.

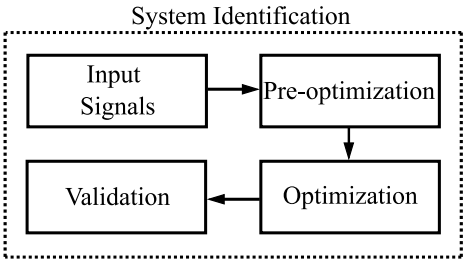


Fig. 1 Flowchart for the proposed system identification process, comprising the four main stages: obtaining the input signals as references, pre-optimization used to define the initial guesses of the parameters, the optimization itself, and validation.

Note that for practical applications of epileptic seizure suppression, the identified state space model is used for designing the controller and state observer, as introduced by [24][17]. Further information is included herein to clarify to the reader.

2.1 Obtaining the Input Signals using Epileptor

Epileptor is a mathematical dynamic model that represents the main features of epileptic seizures, such as fast oscillations and spike or spike and wave events, which are two of the most common features in time signatures of epileptiform activities [15]. Under the premise that dynamic structures in such activities are shared across species, it was developed by Jirsa and colleagues [15] based on an experimental model considering the electrical brain activity of mice. Tools from nonlinear dynamics, as limit cycles, bursters and phase portrait analysis were largely used to propose such a model, whose study led to a taxonomy of seizure-like events depending on the types of bifurcation found in real signals. In this sense, Epileptor presents, according to the same authors, two specific ones: saddle-node bifurcation (for seizure onset) and homoclinic bifurcation (for seizure offset), modeled in terms of local field potentials, usually given in μV. To represent all of these features, a set of six first-order differential equations was proposed, given in state-space notation by:

$$\begin{cases} \dot{\mathbf{x}}(t) = \mathbf{A}\mathbf{x}(t) + \mathbf{b} \\ \mathbf{y}(t) = \mathbf{C}\mathbf{x}(t) \end{cases} \tag{1}$$

where the $\mathbf{A}$, $\mathbf{b}$ and $\mathbf{x}$ are respectively given by

$$\mathbf{A} = \begin{bmatrix} -g_1'(x_1,x_2) & 1 & -1 & 0 & 0 & 0 \\ -5x_1/\tau_1 & -1/\tau_1 & 0 & 0 & 0 & 0 \\ 4/\tau_0 & 0 & -1/\tau_0 & 0 & 0 & 0 \\ 0 & 0 & -0.3 & (1-x_2^2) & -1 & 2 \\ 0 & 0 & 0 & g_2'(x_2)/\tau_2 & -1/\tau_2 & 0 \\ 0.1\gamma & 0 & 0 & 0 & 0 & -\gamma \end{bmatrix} \tag{2}$$

$$\mathbf{b} = \{I_{rest1}\ y_0/\tau_1\ -4x_0/\tau_0\ 1.05 + I_{rest2}\ c/\tau_2\ 0\}^T \tag{3}$$

$$\mathbf{x} = \{x_1\ y_1\ z\ x_2\ y_2\ u\}^T \tag{4}$$

where:

$$g_1'(x_1,x_2) = \begin{cases} x_1^2 - 3x_1, & x_1 < 0 \\ x_2 - 0.6(z-4)^2, & x_2 \geq 0 \end{cases} \tag{5}$$

$$g_2'(x_2) = \begin{cases} 0, & x_2 < -0.25 \\ 6, & x_2 \geq -0.25 \end{cases} \tag{6}$$

$$c = \begin{cases} 0, & x_2 < -0.25 \\ 1.5, & x_2 \geq -0.25 \end{cases} \tag{7}$$

The matrix $\mathbf{C}$ is composed of a linear combination between $x_1(t)$ and $x_2(t)$ (i.e., $-x_1 + x_2$), which is the observable activity $\mathbf{y}(t)$ that can be measured over time:

$$\mathbf{C} = [1\ 0\ 0\ -1\ 0\ 0] \tag{8}$$

A biophysical factor is associated to each of these variables and parameters, which are briefly described as follows [15][17][24]:

First subsystem (x_1 and y_1): this set of variables is responsible for generating the so-called fast oscillations, that is, the activity with the fastest time scale (τ_1) among all of the variables. The measurable activity over time is x_1, whereas the unmeasurable one is given by y_1. Together, both account for the first important dynamic structure in Epileptor, characterized by an inward-spiralling attractor in the phase portrait. They are associated to neuron membrane electrical activity, modeled as local field potentials, which can be given in μV or mV.

Second subsystem (x_2 and y_2): this set of variables, in turn, is responsible for generating spike and wave events, which is an activity with a relatively slower time scale (τ_2) compared to the first set. The measurable activity over time is x_2, whereas the unmeasurable one is represented by y_2. Similarly, they intend to model membrane potentials, given in μV o mV, but their dynamic structure is evidenced by an open limit-cycle constant oscillation.

Permittivity: this entity, represented by $z(t)$, is a control parameter; that is, depending on its values, Epileptor may be driven into or out of a seizure, which accounts for its bi-stable behavior. It is possibly related to slow-evolving extracellular processes that occur during epileptiform activity, such as levels of ions, oxygen and energy metabolism. Its time scale is represented by τ_0. Therefore, the following relation holds: $\tau_0 > \tau_2 > \tau_1$.

Electric currents: I_1 and I_2 represent the flow of electric currents that flow inward or outward neural cells, for the first and second subsystems, respectively.

Epileptogenicity: this entity is modeled by x_0, thus representing the degree of intensity that the seizures described by Epileptor present, in terms of amplitude and duration.

Coupling functions: as discussed in [15], there is evidence that both fast oscillations and spike and wave events are usually coupled. This behavior is thereby captured by the following functions: g_1' and g_2'.

Dummy variable $u(t)$: this variable can be modeled as a differential or integral equation, as demonstrated in [15][22][17]. It does not provide a concrete biophysical meaning, although it works as a low-pass filter due to the time scale separation: $1/\gamma = 100 \gg \tau_2$.

Constant values: y_0 and γ are mathematical constants and do not represent any specific biophysical meaning either, which were introduced by [12] and [15], respectively.

2.2 Pre-optimization

Based on the Epileptor model, note that there is a set of 8 parameters that characterize a local field potential, expressed below as vector $\mathbf{P}$:

$$\mathbf{P} = \{\tau_0,\ \tau_1,\ \tau_2,\ \gamma,\ x_0,\ y_0,\ I_{rest1},\ I_{rest2}\}^T \tag{9}$$

or, using an equivalent notation, for simplicity, $\mathbf{P} = \{p_1,\ ...,\ p_8\}^T$, where $p_1 \equiv \tau_0$ and so forth until $p_8 \equiv I_{rest2}$. Note that all of them must be known before using the Epileptor model. In practice, this means that such a set is patient-specific; that is, each individual presents their unique seizure signature, which, in turn, implies that estimating these parameters leads to the full description of their epileptiform activity, for a given time window recorded over time. Therefore, the pre-optimization stage concerns the definition of initial guesses for each of them. In this case, $\mathbf{P}$ over the optimizations can be described by

$$\mathbf{P}_n = (\mathbf{I} + \delta\mathbf{D}_n)\,\mathbf{P}^{\text{ref}} \tag{10}$$

where $\mathbf{I}$ 8×8 is an identity matrix, $\mathbf{P}^{\text{ref}}$ is the vector of reference values, δ is the disturbance factor and $\mathbf{D}_n$ is the disturbance matrix, which changes for each n-th iteration in the optimization process. $\mathbf{P}_n$ is the input matrix for the n-th iteration. It is such that $\mathbf{P} \equiv \mathbf{P}^{\text{ref}}$ if $n = 0$ (i.e., no iterations are considered). On the other hand, $\mathbf{P}_n \to \mathbf{P}$ if $n \to N$, where N is the defined maximum number of iterations (i.e., $\mathbf{P}_n$ corresponds to the desired vector $\mathbf{P}$).

The reference vector $\mathbf{P}^{\text{ref}}$ can be arbitrarily defined. However, it is recommended to use values typically employed to describe representative epileptic seizures to improve the feasibility of the optimization process. In this sense, without loss of generality, the values used by [15] are considered. The robust

identification is achieved by conveniently computing the disturbance matrix $\mathbf{D}_n$ of each n-th iteration by the following equation

$$\mathbf{D}_n = \frac{diag\,(\mathbf{r}_n)}{\max\,(|\mathbf{r}_n|)} \tag{11}$$

where $diag(\mathbf{r}_r)$ is a diagonal matrix constructed with the elements in the vector $\mathbf{r}_n = \{r_1 \;\; r_2 \;\; r_3 \;\; r_4 \;\; r_5 \;\; r_6 \;\; r_7 \;\; r_8\}^T$, and $\mathbf{r}_n$ is a randomly-generated vector for the n-th iteration. $\max\,(|\mathbf{r}_n|)$ is the highest value in $|\mathbf{r}_n|$. The highest element r_j is obtained in a different position into the diagonal of the matrix $\mathbf{D}_n$. The disturbance factor δ is previously defined considering $\delta > 0$, such that $\delta = 1$ is the maximum percentage of variation admitted to the parameter in $\mathbf{P}_n$ in relation to the reference value in $\mathbf{P}^{\text{ref}}$. For example, if $\delta = 0.25$, $\delta\mathbf{D}_n$ includes 25% of variation in p_j (i.e., the j-th element into $\mathbf{P}_n$) in relation to its reference value defined in $\mathbf{P}^{\text{ref}}$. Figure 2 shows a schematic illustration of this approach, in which D_j is the j-th element from the diagonal of $\mathbf{D}_n$. Note that $D_i < D_j$ $\forall\, i \neq j$.

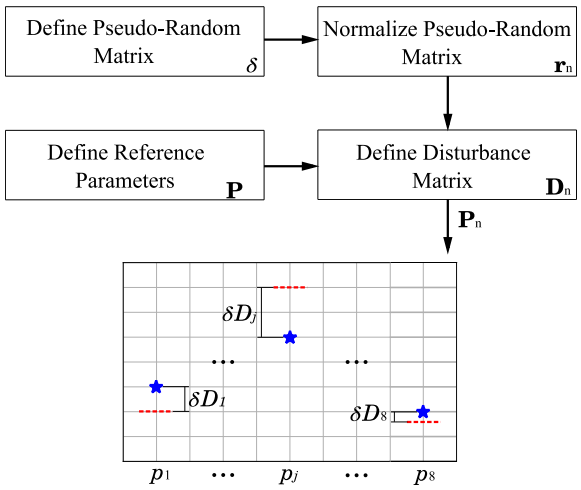


Fig. 2 Visual illustration of the non-null values in $\delta\mathbf{D}_n$. Initially, the uncertainty factor for the optimization is defined as δ, along with the pseudo-random matrix $\mathbf{r}_n$; then, this matrix is normalized by its maximum value, thus leading to the disturbance $\mathbf{D}_n$; at last, the initial guesses $\mathbf{P}_n$ are formed by the disturbance term and the previously defined reference values $\mathbf{P}$. Red dashed lines represent the reference values and $\star$ represents each value of p_j for the n-th iteration.

2.3 Optimization

The optimization process is employed to get $\mathbf{P}_n \rightarrow \mathbf{P}$ from $\mathbf{P}^{\text{ref}}$. Each n-th iteration is evaluated by computing the function $f(W,\; w_n)$, where $W \equiv$

LFP^{ref}, i.e., the target LFP. Similarly, w_n is the LFP obtained by integrating the Epileptor model in the time domain considering the parameters in $\mathbf{P}_n$, i.e., the n-th set of parameters. The function $f(W,\ w_n)$ is defined by

$$f(W, w_n) = \frac{1}{\phi}\left[\frac{1}{K}\sum_{k=1}^{K}\left(W(k) - w_n(k)\right)^2\right]^{1/2} \tag{12}$$

where $W(k)$ and $w_n(k)$ correspond respectively to the k-th value of W and w_n, $k = 1, ...,\ K$, i.e., their discrete representation for computational purposes is considered. $\phi = |W^{\max} - W^{\min}|$, which is a normalization based on the maximum and minimum values of the reference LFP, and K is the number of time instants considered. Note that the target LFP is the reference local field potential to be described using the identified Epileptor model. In practical applications, it is a recording of epileptiform activity, whose parameters are unknown. The optimization procedure is defined as a minimization problem, as follows:

$$\min_{\mathbf{P}_n}\left[f(W,\ w_n)\right] \tag{13}$$

The strategy established in the optimization procedure is as follows: for each n-th iteration, a set of parameters $\mathbf{P}_n$ is evaluated; a computational simulation for the Epileptor model is then run for such a set; in case $f(W, w_n) = 0$, then $w_n \equiv W$, and the iteration process is stopped. Typically $f(W, w_n) = 0$ is not achieved, and because of this, the tolerance value ϵ and the maximum number of iterations N are predefined. Then, it is checked if $f(W, w_n) \leq \epsilon$ to stop the iteration process. Figure 3 shows an illustration of this iteration process.

The Nelder-Mead algorithm was chosen because it provides a good convergence speed [**?**], it is easily addressable, its implementation is relatively simple, and presents a low computational complexity [**?**], which makes it an interesting option, where several successive optimizations are performed, as shown in next section. It has been used for different applications, such as the tuning of Kalman filters [29], or model parameters estimation [**?**][30], for example. This algorithm was first established in 1965 [27] and it is also known as Downhill Simplex Method [**?**].

2.4 Validation

The validation stage comprises repeating the optimization process considering M different time frames to define W. The idea is to evaluate an entire seizure, from preictal to postictal states, by cutting the signal in M parts. According to the number of points measured in the target LFP, it is possible to consider an overlap as usually done in signal processing techniques [**?**]. The M repetitions provide $\mathbf{P}^{(1)}$, ..., $\mathbf{P}^{(M)}$ sets of parameters. The set used is the median resulting value of all optimizations, i.e.,

$$\mathbf{P} = \text{med}\{\mathbf{P}^{(1)}, ...,\ \mathbf{P}^{(m)}, ...,\ \mathbf{P}^{(M)}\} \tag{14a}$$

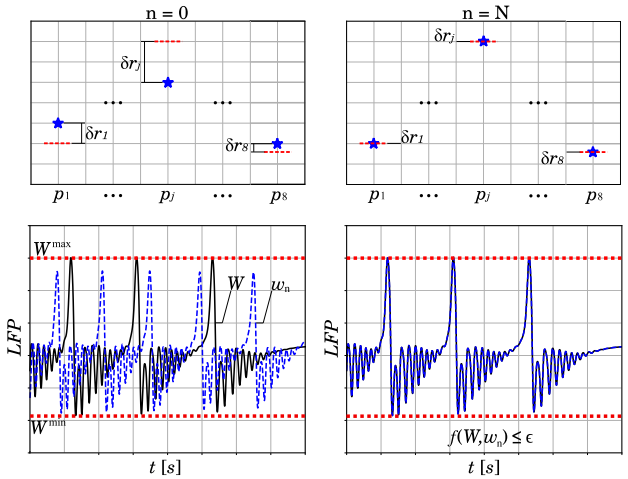


Fig. 3 Visual illustration of the iteration process for a time window of an LFP. Initially, at $n = 0$, both target W and optmized w_n LFPs present different parameters, whose variation is defined by the uncertainty factor δ; as the iterations proceed, this difference is minimized until a maximum number of iterations N or tolerance ϵ is achieved.

There are advantages in doing so, as summarized below:

- depending on the requirements of the optimization (in this case, the number of points, for example), it may take a relatively long time for the parameters to converge towards the desired ones. Therefore, shorter time windows enable to perform several shorter, faster evaluations, which leads to a finer resolution in function of the number of windows applied;
- since preictal, ictal and postictal signals have different characteristics, the best estimate for the parameters can be found individually, for each part, or as a whole, based on median values of multiple successive operations;
- even if a set of parameters proves to be the best fit for a part of the LFP but not for another one, by using median values, all of the parameters yielded from the optimization can be analyzed as independent values and converge to the desired ones. For instance: in case $f_m(W, w_n) > \epsilon$, obtained if the number of iterations exceeds the predefined one or a global minimum that does not tend to zero is achieved for some m, it is possible that one or more of its p_j diverge considerably from p_j^{ref}. Once many time windows are adopted, the overall median result tends to compensate for particular discrepancies like this, because it is supposed to tend towards the target values without being significantly affected by extreme values.

Figure 4 depicts an illustration of this approach, considering sequential time windows over time, based on a reference (i.e., the target) LFP. The frame used herein considered that it is the minimum non-repeating cell for reproducing Epileptor's main stages: interictal and ictal. After the specified number of points, the same structure is obtained over and over, which characterizes the

system's bi-stable behavior [15]. Moreover, by considering such a frame, the transitions between states are also captured during the optimizations.

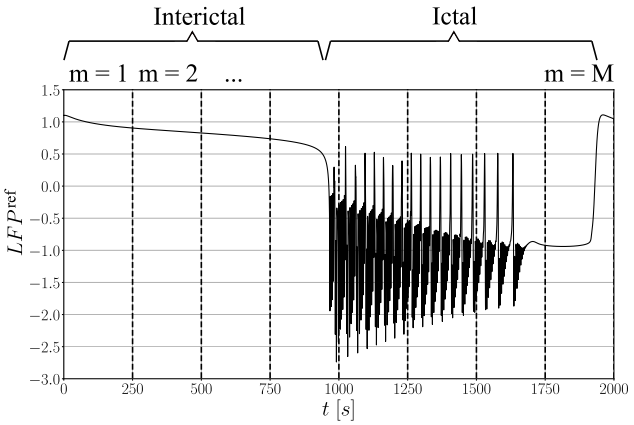


Fig. 4 Validation process for the system identification approach using sequential time windows to estimate the unknown parameters of the target LFP. According to Eq. 14, each window m represents a full optimization process, as described in Section 2.3, leading to a set of parameters $\mathbf{P}^{(m)}$, $m = 1, 2, ..., M$. The final set of parameters, considered the best representative one, is given by $\mathbf{P} = \text{med}\{\mathbf{P}^{(1)}, ..., \mathbf{P}^{(m)}, ..., \mathbf{P}^{(M)}\}$.

Integrating system identification and controllers for seizure suppression

The problems of reconstructing Epileptor's unmeasurable variables based only on the measurable ones for purposes of seizure suppression have been addressed in [24][17]. Essentially, both are related to designing observers and controllers, by computing specific gains for each of the state of the model based on Linear Matrix Inequalities (LMIs) [32][33]. The main idea is to obtain weight matrices $\mathbf{G}$ and $\mathbf{L}$ such that:

$$\dot{\hat{\mathbf{x}}}(t) = \mathbf{A}\hat{\mathbf{x}}(t) + \mathbf{b} - \mathbf{BG}[\hat{\mathbf{x}}(t) - \mathbf{x}_h] + \mathbf{L}[\mathbf{y}(t) - \hat{\mathbf{y}}(t)] \tag{15}$$

where $\hat{\mathbf{x}}$ is the state vector for the copy of the system, $\hat{\mathbf{y}}$ is its associated output, $\mathbf{B}$ is the matrix related to the control input, $\mathbf{x}_h$ is the desired healthy state (to which the controller drives the system after its activation). Note that, with an appropriate choice for $\mathbf{L}$, $\mathbf{y}(t) \to \hat{\mathbf{y}}(t)$, which implies that $\mathbf{L}[\mathbf{y}(t) - \hat{\mathbf{y}}(t)] \to 0$, thus approximating the copy to the original system. Furthermore, as $\mathbf{G}$ is defined, $\hat{\mathbf{x}} \to \mathbf{x}_h$, driving the system to a seizure-free state. It must be stressed that this modeling has been done considering a fuzzy Takagi-Sugeno approach, which aims at obtaining multiple linear subsystems based on an original nonlinear one [33]. However, for clarity of understanding, this step has been omitted from this text. Further details can be found in [17][24].

Figure 5 presents the integration of all the stages mentioned in this work. Two major steps are, thus, expected: an offline/preparation one (I), during which LFPs are acquired (or previously simulated), taken as reference or target signals, and used to design the observer and controller − therefore, note that there must be available data sets, which represent well patients' specific seizure signatures, prior to this stage; and an online one (II), where the gains computed in (I) are already defined and used to reconstruct the unmeasurable variables, thus leading to the full definition of Epileptor's states, necessary to activate the controller − which, in turn, proceeds to deliver the inputs for seizure suppression.

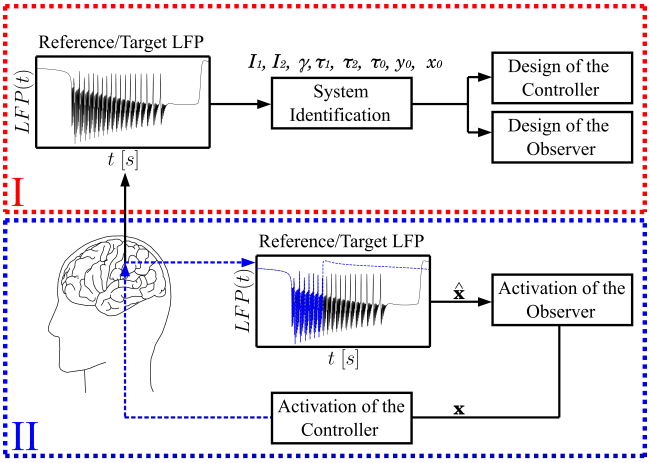


Fig. 5 Integration process considering the proposed system identification technique and seizure suppression. In the offline stage (I), previously acquired LFPs are used as reference signals to carry out the optimization process and obtain the best set of parameters $\mathbf{P}$, as seen in Fig. 4; these values are then used to design both observer and controller. In the online stage (II), the observer is activated to reconstruct Epileptor's actual states $\mathbf{x}$ based on the estimated ones $\hat{\mathbf{x}}$, and the controller uses the reconstructed states to deliver the input stimuli for seizure suppression.

3 Results and Discussion

The proposed approach is evaluated considering a target LFP numerically obtained. An Epileptor model is defined considering the following reference parameters [15]: $\mathbf{P}^{\text{ref}} = \{2857,\ 1,\ 10,\ 0.01,\ -1.6,\ 1,\ 3.1,\ 0.45\}^T$. An example for $\mathbf{P}$ is $\mathbf{P} = \{2142.75,\ 1.1860,\ 12.6744,\ 0.0103,\ -1.3674,\ 1.0436,\ 2.5773,\ 0.4343\}^T$. In particular for this case, note that the main difference is verified for the parameter $\tau_0 = 2142.75$, which is 25% ($\delta = 0.25$) lower than its original value. However, different $\mathbf{P}^{\text{ref}}$ were investigated and similar results were obtained for $\mathbf{P}$. Values of $\epsilon = 10^{-6}$ and $N = 200000$ were set

for the integration in the time domain using the fourth order Runge-Kutta algorithm, with $dt = 0.01$ s.

3.1 Influence of the Time Window

Figure 6 presents the results obtained for the proposed system identification technique using successive optimizations, based on box plots, where the center value is the median ($\mathbf{P}^{\text{best}}$). Note that, as the number of windows gets higher, the values obtained for the parameters tend to approach those originally defined for Epileptor [15] (and chosen in this case), for most of the variables. This is particularly evidenced by how close the reference values are to the medians, despite the variations and number of outliers observed. That is, the general behavior is that the finer the resolution (shorter time windows), the better the results − which is evidenced in Table 1, where the relative mean squared errors (RMSE) between the estimated and actual parameters were calculated, as well as their median final objective-function evaluations (after $M = 800$, 400, 40, 8 and 4 optimizations, respectively, depending on the number of windows).

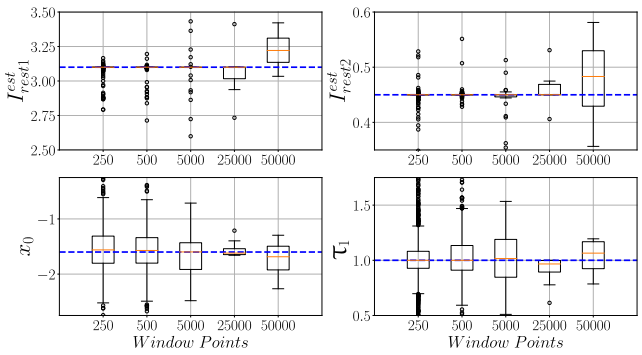


Fig. 6 Estimated parameters for I_{rest1}, I_{rest}, x_0 and τ_1 using different time windows (given in number of points) and $\delta = 0.25$. Blue dashed lines represent the reference values [15].

Table 1 Performance of the optimization approach, in terms of the relative mean squared error (RMSE), for different time windows, considering median values between the estimated ($\mathbf{P}^{\text{best}}$) and reference ($\mathbf{P}^{\text{ref}}$) parameters, and associated median final objective-function evaluations ($f^{\text{best}}(W, w)$).

Window (points)	250	500	5000	25000	50000
RMSE (%)	0.63	1.21	0.66	3.96	1.47
$f^{\text{best}}(W, w)$	$1.32.10^{-6}$	$5.83.10^{-6}$	$2.36.10^{-4}$	$5.5.10^{-2}$	$1.1.10^{-1}$

This is possibly due to the pseudo-random characteristic of the initial guesses: since an unknown combination of them is set at the beginning of

the process, slightly higher or lower values are likely to be obtained for the parameters; also, a set of parameters that best fits one time window is not necessarily the best choice for the remaining ones; however, the guesses tend to converge towards the correct values on average, as the number of available signal samples increases. Furthermore, note that, for this particular case, to obtain an RMSE lower than 1%, the threshold that relates the RMS of an LFP $f^{\text{best}}(W, w) \leq \epsilon$ must be such that $\epsilon = 10^{-6}$.

3.2 Influence of Interictal and Ictal States

In Figure 7, the same parameters as in Fig. 6 are shown over the number of optimizations (alternatively, the number of time windows), but using a 250-point frame. For the parameters chosen, different characteristics are observed over the number of optimizations (which include information about the LFP over time). For I_{rest1}, the estimated values remain at an almost unchanged baseline, thus providing an accurate representation of its original magnitude. Such a parameter is only present in vector **b** in Epileptor's equations, which is decoupled from the dynamic matrix, which might be why it is relatively easier to be approximated (the same behavior occurred for I_{rest2}).

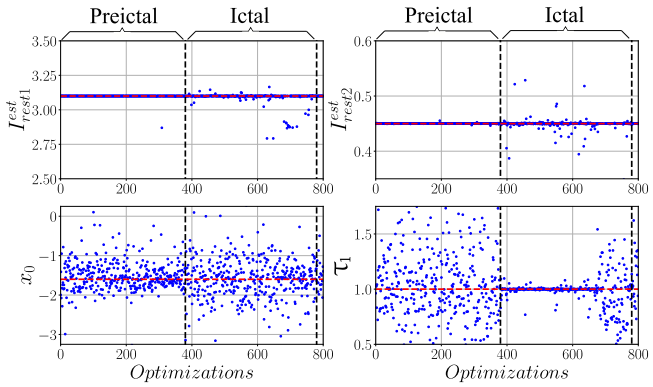


Fig. 7 Parameters I_{res1}, I_{rest}, τ_1 and x_0 for a finer resolution, using a 250-point time window, comparing the preictal and ictal states. Dashed red lines represent the reference values. Vertical dashed lines represents transitions of states.

As for x_0, two possible reasons may be associated with its behavior: it interacts with other parameters that must be estimated (as τ_0, for example), which makes it difficult for the algorithm to yield a precise value throughout the whole signal; besides, it is associated with variable $z(t)$, which represents processes that evolve slowly in time. Note that, for τ_1, the opposite behavior is obtained, probably because it is associated (and interacts) with fast-evolving variables and parameters, as x_1 and y_0, respectively. Therefore, each of the parameters are better estimated according to their biophysical nature in terms

of time scale. Furthermore, this endorses the fact that adopting successive optimizations, including interictal and ictal states, is an interesting strategy, even if the resulting values must be averaged.

This result can be generalized, as seen in Figures 8 and 9, where a comparison between the box plots in the interictal and ictal states is presented. Note that, for the parameters x_0, τ_0, which are related to variables that evolve in a slower time scale, their best estimation is performed before a seizure occurs; whereas for the parameters y_0, τ_1, and τ_2, which are related to variables that evolve in a faster time scale, an opposite behavior takes place. Parameters I_{rest1} and I_{rest2} are exceptions; however, as mentioned before, their values do not belong to the dynamic matrix, and the results for the interictal period are fairly good and do not significantly compromise their estimation.

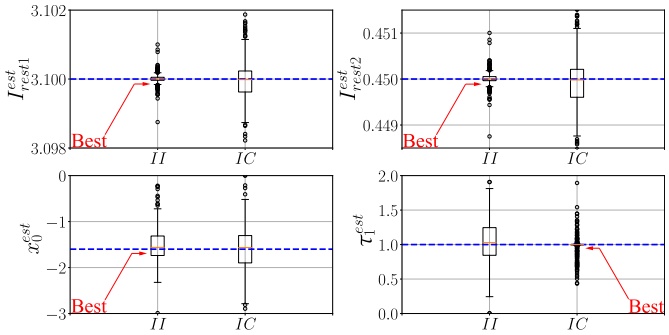


Fig. 8 Comparison between interictal (II) and ictal (IC) states using the box plots of parameters I_{rest1}, I_{rest2}, x_0 and τ_1, and a 250-point time window. Dashed blue lines represent the reference values.

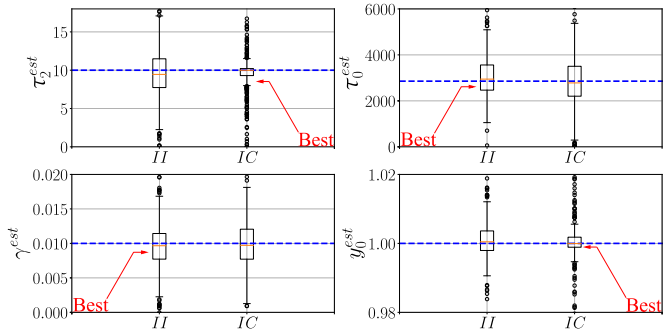


Fig. 9 Comparison between interictal (II) and ictal (IC) states using the box plots of parameters τ_2, τ_0, γ and y_0, and a 250-point time window. Dashed blue lines represent the reference values.

As a general rule for deciding which periods of time during an LFP activity described by Epileptor should be measured for the best possible estimation of its parameters, that is, which parts of the signal over time are more likely to provide the right estimates, arrows pointing to the best box plot are indicated in both Figs. 8 and 9. Essentially, the criterion used is not only how close the median values are to the reference once, but the variation around them: low fluctuations imply in higher chances of estimating the correct values. Parameter γ, linked to the dummy variable $u(t)$, presented a slightly better result for the interictal state; however, since it is not directly related to any biophysical entity and works as a low-pass filter, it can be reasonably estimated in both regions, as seen in the same figure.

3.3 Influence of the Uncertainty Factor δ

Figure 10, in turn, depicts a comparison between the estimated parameters obtained for different uncertainty factors δ. Note that, as the uncertainty (that is, the relative distance between the estimated and actual values) increases, the parameters tend to move farther from the reference ones. This is particularly evidenced by the increase in variation around the median values – which, however, are still fairly close to the target ones. In practical terms, the prior lack of information about the initial guesses influences directly on the final output; that is, the less, the worse. Nonetheless, accurate predictions can be made based on the successive optimizations method. At last, Table 2 summarizes these results, showing that not only does the relative mean square error get higher with the uncertainty, but also that the final objective-function evaluation is farther from zero.

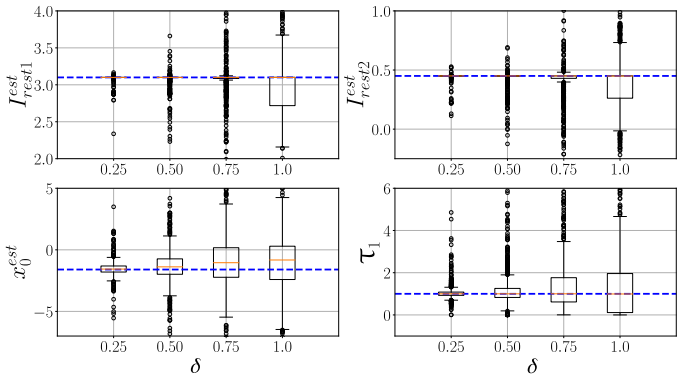


Fig. 10 Estimated parameters for I_{rest1}, I_{rest}, x_0 and τ_1 using different uncertainty factors δ and a 250-point time window. Blue dashed lines represent the reference values.

Table 2 Performance of the optimization approach, in terms of the relative mean squared error (RMSE), for different uncertainty factors δ, considering median values between the estimated ($\mathbf{P}^{\text{best}}$) and reference ($\mathbf{P}^{\text{ref}}$) parameters, and associated median final objective-function evaluations ($f^{\text{best}}(W, w)$).

δ (%)	25	50	75	100
RMSE (%)	0.63	4.47	12.40	16.43
$f^{\text{best}}(W, w)$	$1.32.10^{-6}$	$1.71.10^{-5}$	$5.22.10^{-4}$	$3.1.10^{-3}$

3.4 Suppressing seizures based on estimated parameters

As illustrated in Fig. 5, after carrying out the system identification methodology proposed in this work, the first requirement for applying observers and controllers is met: since both rely on knowing the initially unknown parameters before being designed, once these values are available, the necessary respective gains, for reconstructing the Epileptor's model and driving it out of a seizure [24][17], can be properly computed. Therefore, the following strategy for seizure suppression is adopted: the estimated parameters are directly used to design both controllers and observers; the gains obtained from the design are then used along with inputs to each of the states of the system, which characterizes the state feedback control approach [17]. Note that the design step is performed with estimated parameters, whereas the activation of both observer and controller is for the real system, with the actual values of the parameters. It is expected thus that, albeit the set $\mathbf{P}^{\text{best}}$ is different from the real condition, it is sufficiently close to it.

Figure 11 presents the aforementioned strategy, including the reference LFP (W) and the resulting one (w) after the successive optimization process, constructed with the estimated values using a 250-point time window and $\delta = 0.25$. Note that the curves present a good fit, and the only major visual difference is related to a horizontal stretch from both sides, leading to a positive delay over time. Nonetheless, such a discrepancy does not significantly compromise the controller's performance: as soon as it is activated, it can efficiently drive Epileptor out of a seizure, back to the healthy condition, expressed by the baseline at a higher LFP level.

It is worth mentioning that, although the relative mean square error for this condition is around zero ($RMSE = 0.63\%$, from Table 1) and the difference between the expected output signal and the target one is slight, it can still be visually well identified. This suggests that the threshold ϵ must be as low as possible for an accurate estimation of Epileptor's parameters to be made. Due to this fact, close attention should be paid to those whose variation affect significantly slow-evolving processes in the time domain and, thus, are directly related to driving Epileptor into and out of seizures: x_0 and τ_0. Mathematically [34] and phisically [15] speaking, $z(t)$ is a control variable, which explains this behavior, and since it presents both of these parameters linked together (as in Eq. 2), it might difficult for the optimization to yield highly precise values. Nonetheless, these results highlight that both interictal and ictal states are relevant when applying system identification approaches.

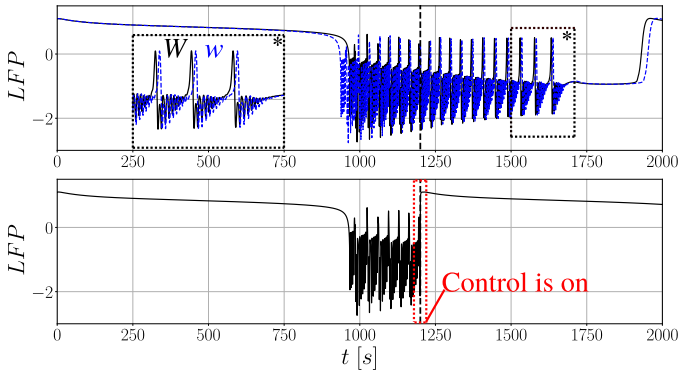


Fig. 11 Comparison between the reference LFP (W) and the one using the estimated parameters obtained from the optimization process proposed in this work (w), as well as the controller's action, over time. The control is activated at 1200 seconds, as indicated by the vertical dashed lines, and kept on for 10 seconds, indicated by the red dotted box, based on the estimated states reconstructed by the observer.

4 Final Remarks

This work has addressed two relevant challenges involving the Epileptor model: *i*) estimating its parameters based on a reference (target) LFP: by using a successive optimization technique, which characterizes a system identification approach, it was possible to obtain their values with a good accuracy, thus leading to the reconstruction of the signal in the time domain; *ii*) integrating this approach with existing methodologies for designing observers and controllers that aim at estimating Epileptor's states and providing input stimuli that suppress its seizures. For the latter one, since such a design relies on knowing the parameters that describe a seizure in the model, its application would be restricted without the contributions achieved in this work.

Considering the different conditions covered herein, the following results were observed: a finer resolution in time (assessed using variable size time windows) may entail a better estimation; both Epileptor's interictal and ictal periods must be taken into account when applying system identification techniques because, as a general behavior, the parameters related to slow-evolving variables are better estimated before seizure onset (interictal period), and the ictal period is a more suitable choice when estimating those associated with fast-evolving variables; as the uncertainty (denoted as δ in terms of percentage) concerning the initial guesses of the parameters increases, the identification process becomes less accurate, which nonetheless does not severely compromise the identification for most of the cases evaluated in this work.

As a consequence, the uncertainty factor, when set to a considerably different value from the reference once, might lead to a higher RMSE. As analyzed in the previous section, this error must be as close to zero as possible for an accurate representation of the parameters to be achieved, otherwise distorted versions of the target LFP may be obtained, which might compromise the

design of the observers and controllers and, consequently, seizure suppression. Therefore, defining boundaries within which each parameter can vary is necessary, as carried out in this work. In practice, it is not possible to measure such boundaries beforehand; however, works addressing variations on the parameters exist in the literature [18][20] and may be useful for establishing references for the initial guesses, which is a major requirement for the optimization process to work properly and lead toward a more rapid convergence.

At last, the integration between the system identification technique with observers and controllers has provided evidence that, once the initially unknown parameters that describe a seizure over time are available, they can be used to design the gains for both, thus leading to an efficient input stimuli application and, consequently, seizure suppression. Testing this strategy with real data may lead to feasible feedback control paradigms in the field of epilepsy, thus contributing to reducing its severe undesired effects and increasing patients' quality of life.

Acknowledgments

The authors would like to thank São Paulo State University (UNESP), School of Engineering of Ilha Solteira (FEIS), Federal University of São Paulo (UNIFESP) and the Group of Intelligent Materials and Systems (GMSINT). The first author thanks to Coordination for the Improvement of Higher Education Personnel (CAPES) for the financial support, Grant Number 88887.481049/2020-00.

Declarations

Funding

This work was funded by Coordination for the Improvement of Higher Education Personnel (CAPES), Grant Number 88887.481049/2020-00.

Conflict on Interests

None declared.

Availability of Data and Material

Not applicable.

Code Availability

The codes for the otimization procedure and the Epileptor model can be found on GitHub at the following address: https://github.com/lheureduloup/epileptor. Two files are used for this purpose: `epileptor_optimization_1.py` (main one) and `epileptor_optimization_2.py` (to generate a reference Epileptor response).

Authors' contributions

J.A.F.B. carried out the simulations and wrote the paper; J.F. and D.D.B. wrote and revised the paper.

Ethics approval

Not applicable.

Consent to participate

Not applicable.

Consent for publication

Not applicable.

References

1. Iasemidis, L. D. Epileptic seizure prediction and control, *IEEE T. on Bio-med. Eng.* **50**(5) (2003) 549–558.
2. Zhu, D., Bieger, J., Molina, G. G. & Aarts, R. M. A survey of stimulation methods used in SSVEP-based BCIs, *Comp. Intel. Neurosc.* (2010) 1–13.
3. Vezzani, A., French, J., Bartfai, T. & Baram, T. Z. The role of inflammation in epilepsy, *Nat. Rev. Neurol.* **7**(1) (2011) 31.
4. Browne, T.R. & Holmes, G.L. *Handbook of epilepsy*, (Lippincott Williams & Wilkins-Philadelphia, Pennsylvania, 2008).
5. Fisher, R. S. & Schachter, S. C. The postictal state: a neglected entity in the management of epilepsy, *Epilepsy Behav.* **1**(1) (2000) 52–59.
6. Walker, J. E., & Kozlowski, G. P. Neurofeedback treatment of epilepsy. *Child and Adolescent Psychiatric Clinics*, **14**(1), 163-176 (2005).
7. D'Andrea Meira, I., Romão, T. T., Pires do Prado, H. J., Krüger, L. T., Pires, M. E. P. & da Conceição, P. O., Ketogenic diet and epilepsy: what we know so far, *Front. Neurosci-Switz.* (13) (2019) 5.
8. Wendling, F., Benquet, P., Bartolomei, F., & Jirsa, V., Computational models of epileptiform activity, *Journal of neuroscience methods* **260** (2015) 233-251.
9. Hodgkin, A. L. & Huxley, A. F. A quantitative description of membrane current and its application to conduction and excitation in nerve, *J. Physiol.-London* **117**(4) (1952) 500–544.

10. FitzHugh, R. Impulses and physiological states in theoretical models of nerve membrane, *Biophys. J.* **1**(6) (1961) 445–466.
11. Morris, C. & Lecar, H. Voltage oscillations in the barnacle giant muscle fiber, *Biophys. J.* **35**(1) (1981) 193–213.
12. Hindmarsh, J. L. & Rose, R. M. A model of neuronal bursting using three coupled first order differential equations, *P. Roy. Soc. Lond. B. Bio.* **221**(1222) (1984) 87–102.
13. Izhikevich, E. M. Simple model of spiking neurons, *IEEE T. Neural Networ.* **14**(6) (2003) 1569–1572.
14. Grimbert, F. & Faugeras, O. Bifurcation analysis of Jansen's neural mass model, *Neural Comput.* **18**(12) (2006) 3052–3068.
15. Jirsa, V. K., Stacey, W. C., Quilichini, P. P., Ivanov, A. I. & Bernard, C. On the nature of seizure dynamics, *Brain* **137**(8) (2014) 2210–2230.
16. Chizhov, A. V., Zefirov, A. V., Amakhin, D. V., Smirnova, E. Y. & Zaitsev, A. V. Minimal model of interictal and ictal discharges epileptor-2, *PLoS Comput. Bio.* **14**(5) (2018) 1–25.
17. Brogin, J. A. F., Faber, J., & Bueno, D. D. An Efficient Approach to Define the Input Stimuli to Suppress Epileptic Seizures Described by the Epileptor Model, *Journal of Neural Systems* (2020) 2050062-2050062.
18. El Houssaini, K., Ivanov, A. I., Bernard, C. & Jirsa, V. K. Seizures, refractory status epilepticus, and depolarization block as endogenous brain activities, *Phys. Rev. E* **91**(2015) 010701.
19. Proix, T., Bartolomei, F., Guye, M. & Jirsa, V. K. Individual brain structure and modeling predict seizure propagation, *Brain* **140**(3) (2017) 641–654.
20. Zhang, H. & Xiao, P. Seizure dynamics of coupled oscillators with epileptor field model, *Int. J. Bifurcat. Chaos* **28**(03) (2018) 1850041.
21. Pinheiro D. J., Oliveira L. F., Souza I. N., Brogin J. A. F., Bueno D. D., Miranda I. A., Da Poian A. T., Ferreira S. T., Figueiredo C. P., Clarke J. R. & Cavalheiro E. A. Modulation in phase and frequency of neural oscillations during epileptiform activity induced by neonatal Zika virus infection in mice, *Scientific Reports* **10**(1) (2020) 1-14.
22. Nagaraj, V., Lamperski, A. & Netoff, T. I. Seizure control in a computational model using a reinforcement learning stimulation paradigm, *Int. J Neural Syst.* **27**(07) (2017).
23. Ichalal, D., Arioui, H. & Mammar, S. Observer design for two-wheeled vehicle: A Takagi-Sugeno approach with unmeasurable premise variables, in: *2011 19th Mediterranean Conference on Control & Automation (MED)*, eds. IEEE, (2011), pp. 934–939.
24. Brogin, J. A. F., Faber, J., & Bueno, D. D. Burster reconstruction considering unmeasurable variables in the Epileptor model, *Unpublished*.
25. Nowak, R. D. Nonlinear system identification. *Circ. Syst. Signal Pr.*, **21**(1) (2002) 109–122.
26. Noël, J. P., & Kerschen, G. Nonlinear system identification in structural dynamics: 10 more years of progress. *Mech. Syst. Signal Pr.* **83** (2017), 2–35.
27. Nelder, J. A., & Mead, R. A simplex method for function minimization. *The computer journal*, **7**(4) (1965) 308-313.
28. Neto L. A., Erasme D., Genay N, Chanclou P., Deniel Q., Traore F., Anfray T., Hmadou R. & Aupetit-Berthelemot C. Simple estimation of fiber dispersion and laser chirp parameters using the downhill simplex fitting algorithm. *Journal of Lightwave Technology*, **31**(2) (2012) 334–342.
29. Powell, T. D. Automated tuning of an extended Kalman filter using the downhill simplex algorithm. *Journal of Guidance, Control, and Dynamics*, **25**(5) (2002) 901–908.
30. Hardt, M., Schraknepper, D. & Bergs, T. Investigations on the Application of the Downhill-Simplex-Algorithm to the Inverse Determination of Material Model Parameters for FE-Machining Simulations. *Simulation Modelling Practice and Theory*, **107** (2021) 102214.
31. Oppenheim, A. V., Willsky, A. S. & Nawab, H. S. *Signals and Systems*, (Prentice Hall-New Jersey, 1997).
32. Boyd, S., El Ghaoui, L., Feron, E. & Balakrishnan, V. *Linear Matrix Inequalities in System and Control Theory*, (SIAM-Philadelphia, Pennsylvania, 1994).
33. Tanaka, K. & Wang, H. O. *Fuzzy control systems design and analysis: a linear matrix inequality approach*, (Wiley-New York, New York, 2004).
34. Slotine, J.-J. E. & Li, W. *Applied Nonlinear Control*, (Prentice hall-Englewood Cliffs, New Jersey, 1991)

Figures

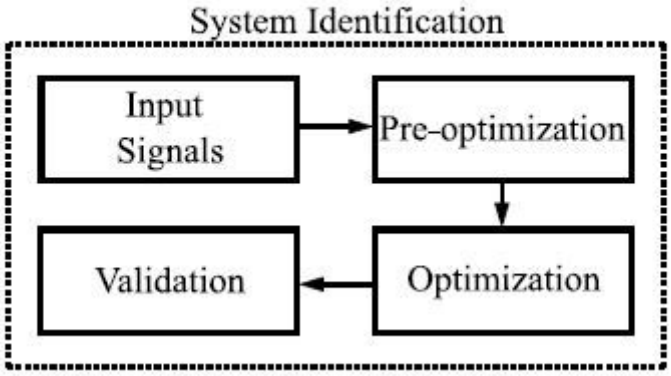


Figure 1

Flowchart for the proposed system identication process, comprising the four main stages: obtaining the input signals as references, pre-optimization used to define the initial guesses of the parameters, the optimization itself, and validation.

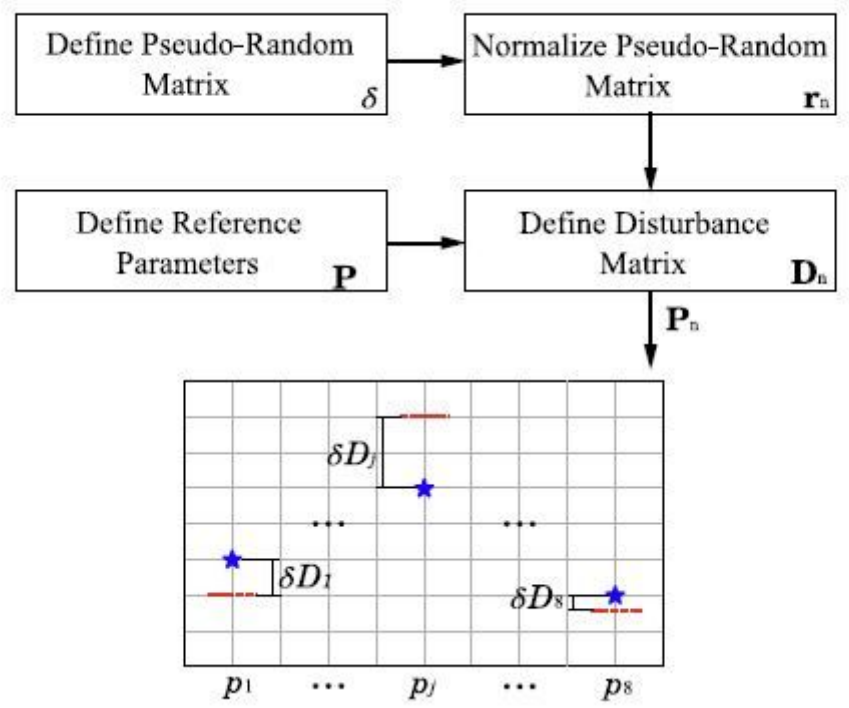


Figure 2

Please See the Manuscript File for the complete figure caption.

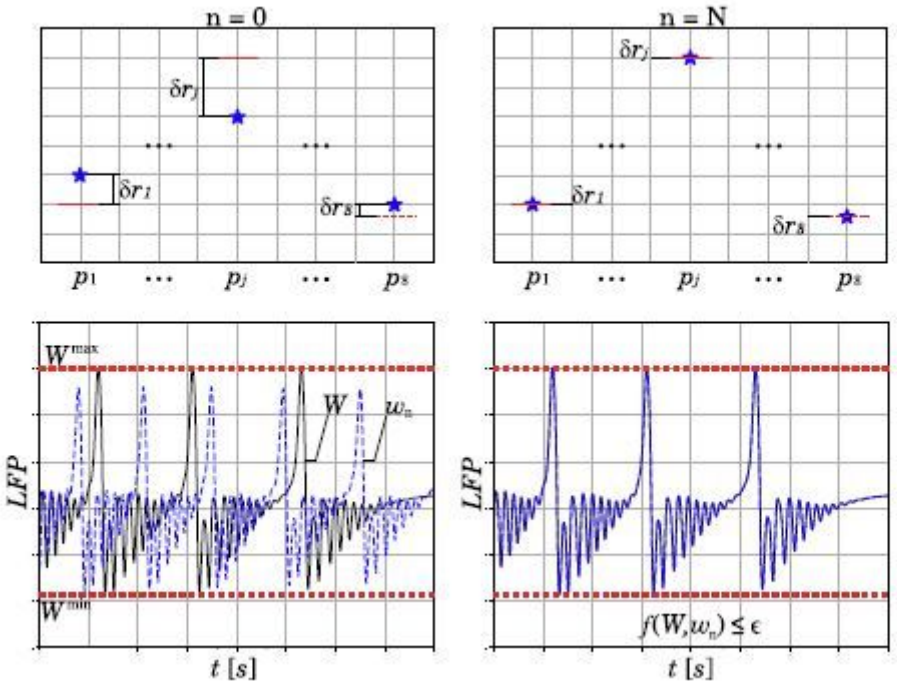


Figure 3

Please See the Manuscript File for the complete figure caption.

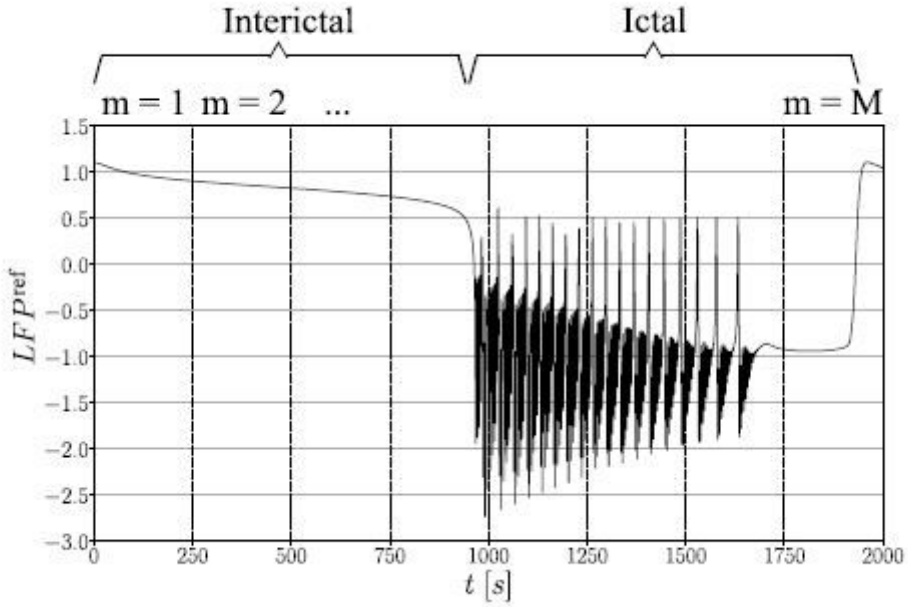


Figure 4

Please See the Manuscript File for the complete figure caption.

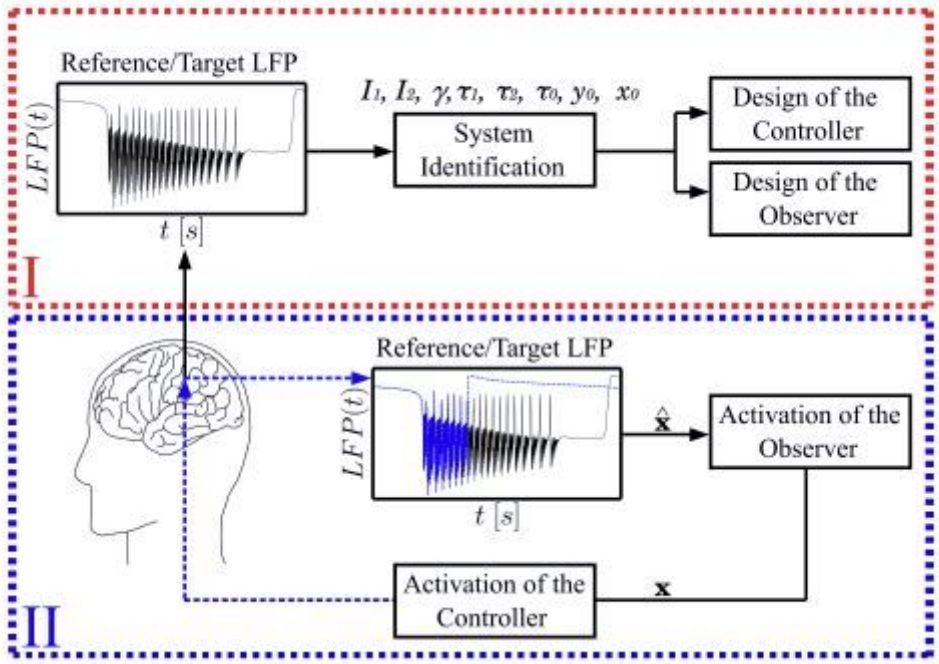


Figure 5

Please See the Manuscript File for the complete figure caption.

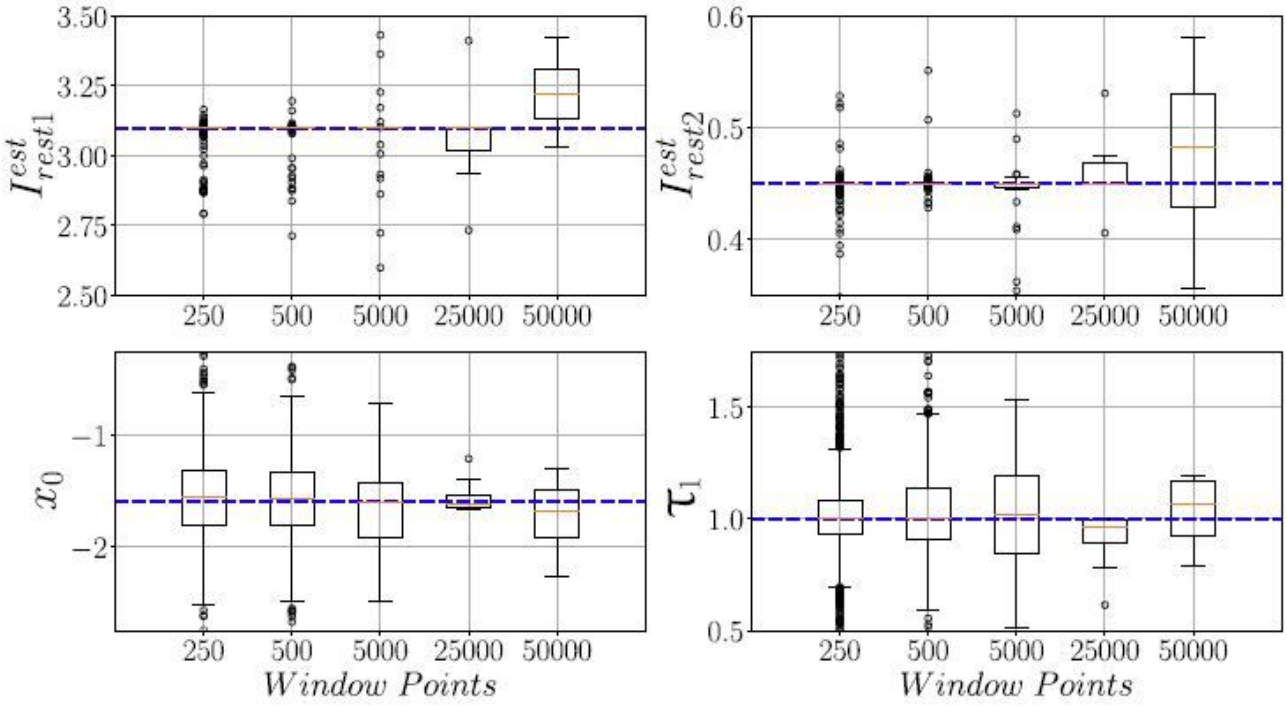


Figure 6

Please See the Manuscript File for the complete figure caption.

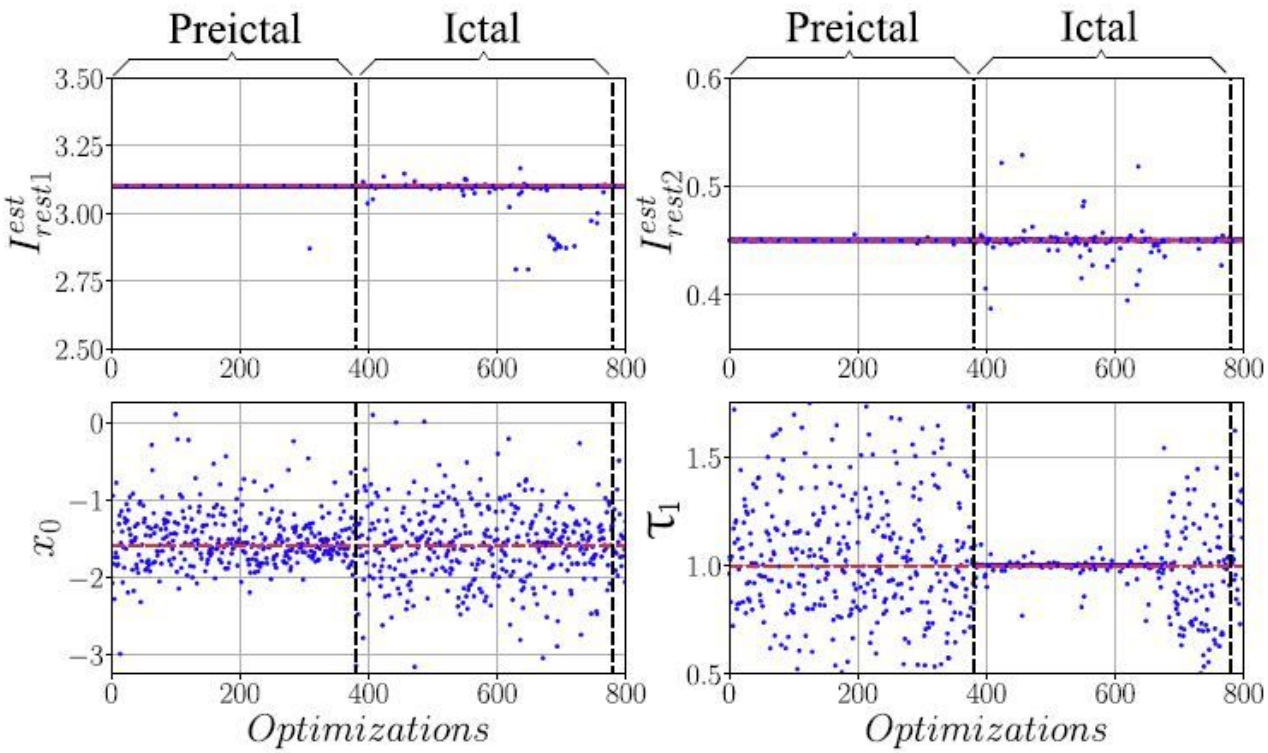


Figure 7

Please See the Manuscript File for the complete figure caption.

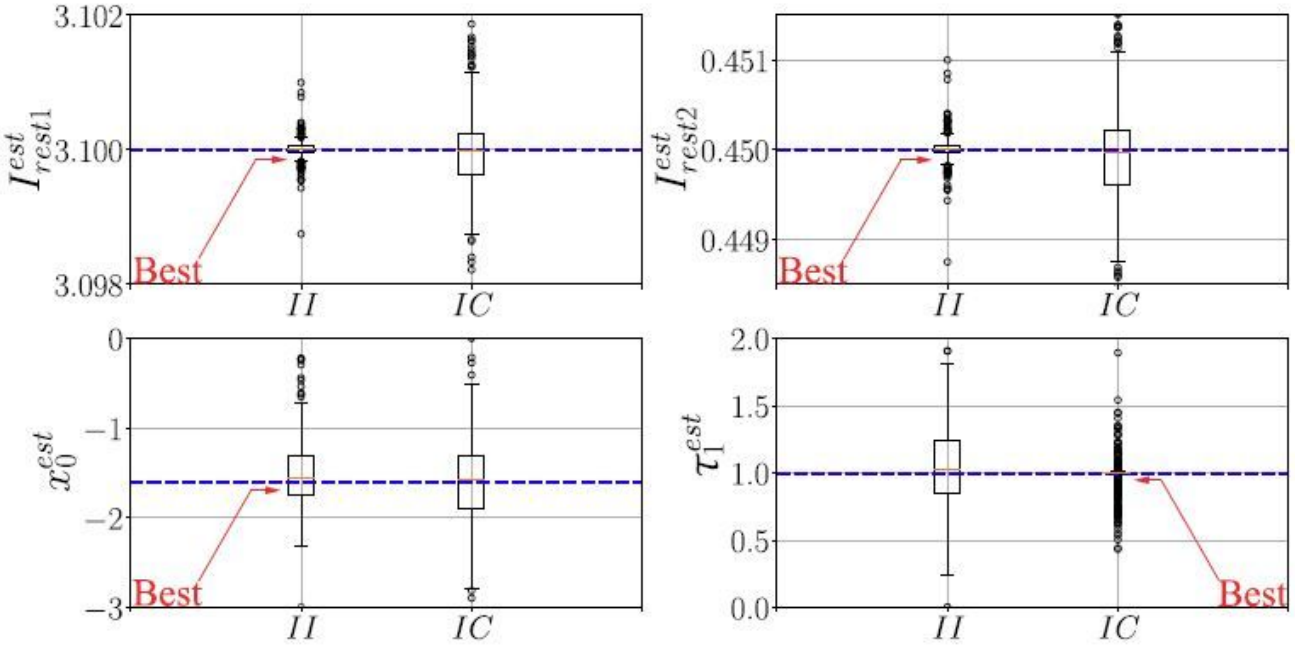


Figure 8

Please See the Manuscript File for the complete figure caption.

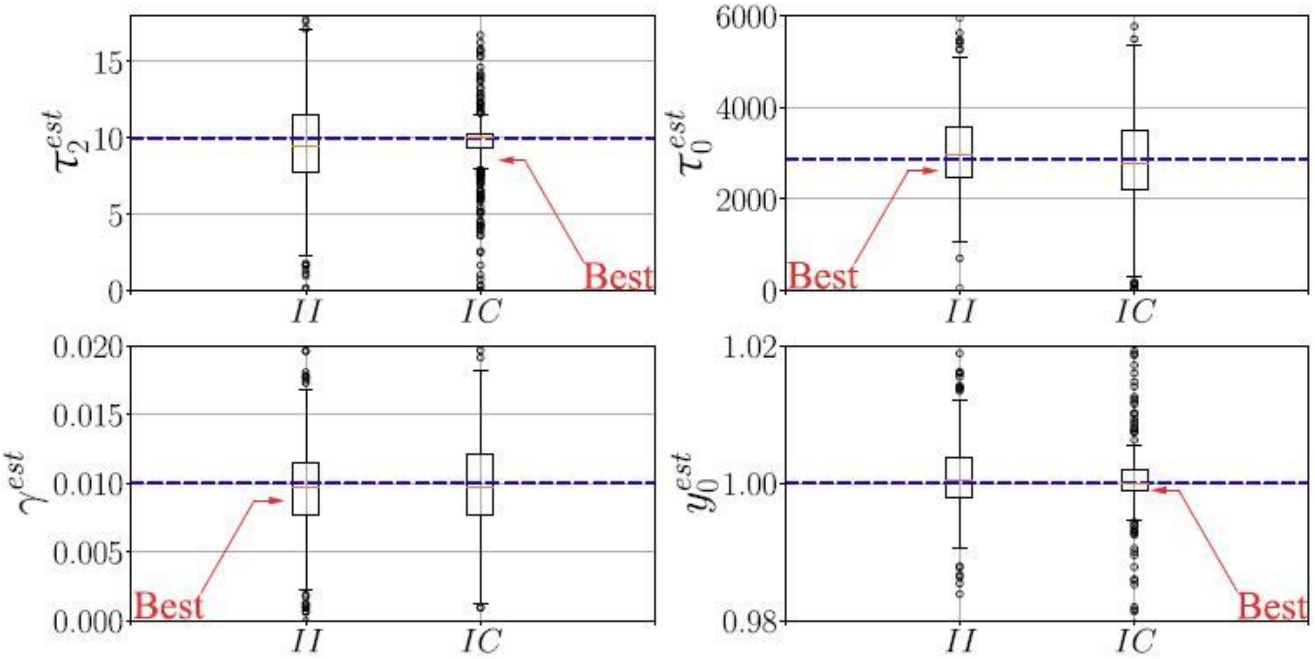


Figure 9

Please See the Manuscript File for the complete figure caption.

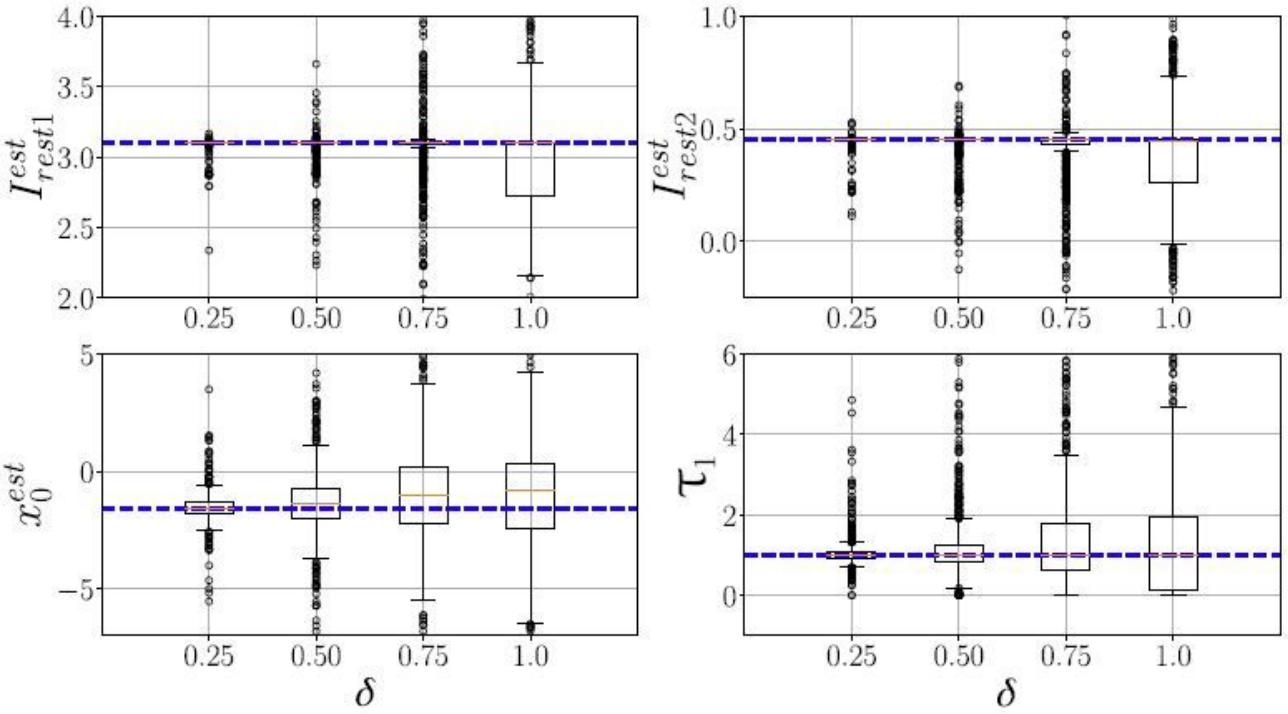


Figure 10

Please See the Manuscript File for the complete figure caption.

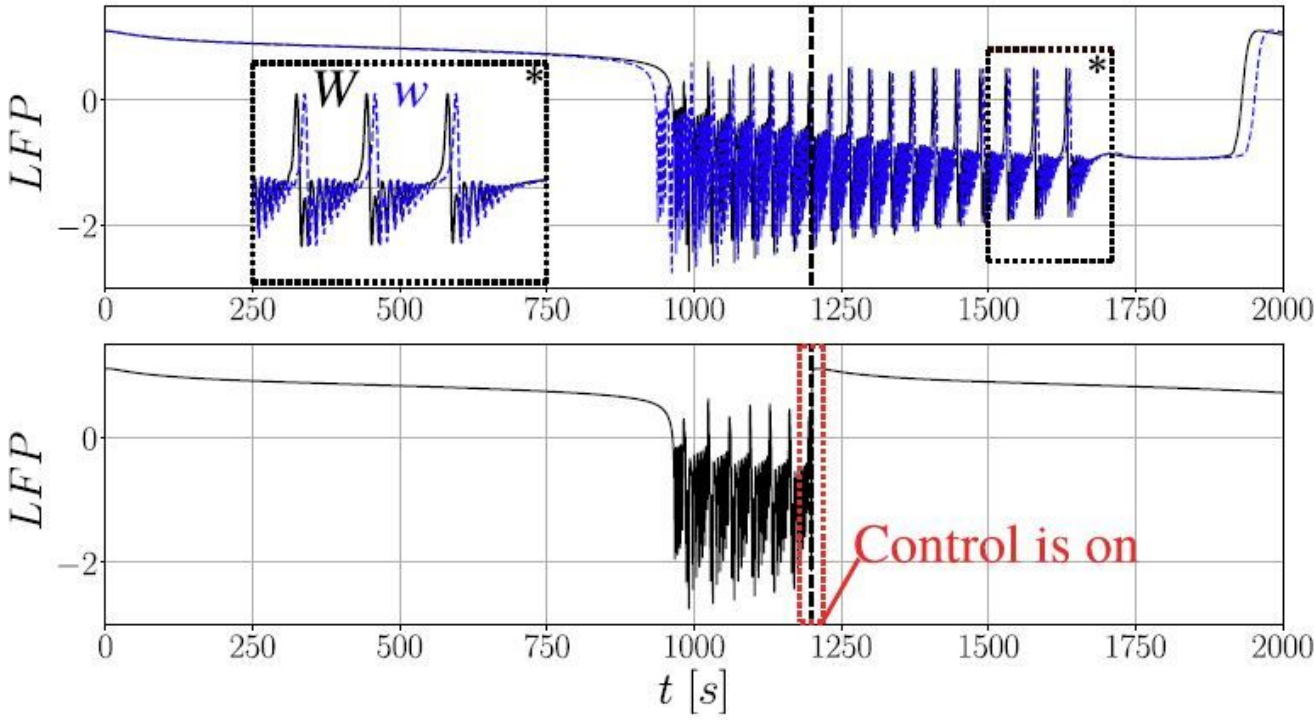


Figure 11

Comparison between the reference LFP (W) and the one using the estimated parameters obtained from the optimization process proposed in this work (w), as well as the controller's action, over time. The control is activated at 1200 seconds, as indicated by the vertical dashed lines, and kept on for 10 seconds, indicated by the red dotted box, based on the estimated states reconstructed by the observer.